ISSN 1330-3651 (Print), ISSN 1848-6339 (Online)
https://doi.org/10.17559/TV-20231231001240
Original scientific paper

A Novel Microwave Imaging Approach Using Rectangular Antenna with Complementary Split-Ring Resonator

M. FAHMITHA BANU*, B. ARUNA DEVI

Abstract: This research addresses the significant issue of breast cancer affecting millions of women worldwide, emphasizing the critical role of early detection in successful treatment. Among various medical technologies, microwave imaging stands out as an efficient and user-friendly method for breast cancer detection, with the antenna being a key component. In this paper, a novel rectangular antenna embedded with a complementary split-ring resonator is proposed for breast cancer detection. The antenna is fabricated using a jean substrate with dimensions of 20 × 15 × 2 mm³. Notably, the proposed antenna demonstrates a wide bandwidth ranging from 2 to 10 GHz. The study introduces the concept of Specific Absorption Ratio (SAR), a measure of how much energy breast tissue absorbs in watts per kilogram (W/kg). The segment aims to highlight the utility of maximum SAR values in identifying the position of tumors within the breast. Through analysis at different frequencies, such as 2.01 GHz and 5.88 GHz, the maximum SAR coordinates closely correspond to the tumor location (–0.75, –2, 0). This indicates that the maximum SAR value is higher in the breast phantom with a tumor compared to the breast without a tumor, showcasing the potential of the proposed antenna for accurate tumor localization. The designed antenna is not only fabricated but also measured. Its notable features include multiband operation, compact size, stable radiation pattern, and a gain exceeding 3.25 dBi across the entire resonating band. These attributes make the antenna well-suited for applications in breast cancer imaging and wireless body area networks (WBAN) within the ISM band. Overall, the presented research contributes to the advancement of microwave imaging technologies for early breast cancer detection and monitoring.

Keywords: complementary split ring resonator (CSRR); multiband frequency; return loss –|S11|; SAR (Specific Absorption Ratio); textile antenna

1 INTRODUCTION

Deadly diseases are rising due to unhealthy living habits and toxic environments, resulting in high death rates. The only way to live healthily is to do regular health check-ups and diagnose deadly diseases early. To carry out routine health check-ups without visiting hospitals in person, a doctor can use a bio-telemetry technique to diagnose the patient. The study of data communication for medical purposes is called biotelemetry. This involves monitoring the vital signs of patients or a person under study and sending the information to a doctor or health care unit remotely. In bio-telemetry, microstrip patch antennas [31, 32] have recently gained much attention. In the current era, bio-telemetry replaces long hospital stays where patients do not need to consult their doctors in person. In addition to monitoring a patient's medical data in the home, this system facilitates diagnosis, treatment, disease prediction, and management of the condition [1]. Biocommunication systems can be created by implanting antennas into the body or mounting them over the torso (skin, fat, muscle) between medical devices and external instruments [1]. Thus, antenna selection is crucial to wireless biotelemetry in health monitoring systems [2]. A variety of medical applications use antennas, including hyperthermia, cancer treatment, tumor detection, and head and neck cancer treatment, as well as remote health monitoring, speech sensing, self-monitoring, digestion monitoring, and brain activity monitoring [3]. Several antennas have been designed for biomedical applications in past research work, like blood glucose monitoring [4, 5], blood pressure monitoring [6, 7], brain tumor detection [8-11], Cancer detection [12-15] etc. Among all the diseases, cancer is considered one of the deadliest diseases, which can be treated and cured when diagnosed earlier. It is estimated that there are more than 100 types of cancer in the world, according to the National Cancer Institute [16, 17]. Around the world, breast cancer is the most common malignancy among women. It is the leading cause of global cancer incidence in 2020. In recent years, it has overtaken lung cancer in terms of new cases, with an estimated 2.3 million or 11.7% of the total number of cancers worldwide [18]. According to epidemiological studies, breast cancer is globally expected to affect more than two million people by 2030 [19]. According to statistics, there were 118000 incidents in India in 2016 (95% uncertainty interval, 107000 to 130000), of which 98.1% of the victims were female, and 526000 cases (474000 to 574000) were prevalent. A Globocan study found that 13.5% (178361) of cancer cases in India are due to Breast Cancer, and 10.6% (90408) are due to other cancers [20]. The American Cancer Society reported that more than 43250 women would die of breast cancer in 2022. In addition, it is estimated that more than 287250 new cases of invasive breast cancer will be diagnosed among women in the United States. Breast cancer must be detected early, and the exact location and size of the tumor are vital. In an early-stage tumor, the cells are very small and can be located using microwave imaging. There is currently an X-ray mammography technique used to detect tumors. However, the results may be inaccurate because of the density of the patient's breasts and the radiologist's expertise in conducting the test and analyzing the data. In this technique, the malignancy of cancerous cells may not be detected in women below 50 years due to the denser density of breast tissue. The denser density of breast tissue will be white, making it difficult for radiologists to distinguish between healthy and cancerous tissue [21]. Another technique to detect tumors is the biopsy method. The purpose of a breast biopsy is to obtain a sample of breast tissue for testing. A pathologist (a doctor who analyses blood and body tissue) examines a tissue sample in a lab to determine a diagnosis. Pathologists prepare pathology reports that describe the size, consistency, and location of biopsy samples. Reports provide information about whether cancerous or non-cancerous changes and precancerous cells were present. A surgical biopsy is recommended if only healthy tissue or benign breast changes are detected in the pathology report, even though

cancer tissue is still present. In addition, a surgical biopsy is expensive, time-consuming, and painful and may lead to false results if tissue is removed from the wrong area. Breast Ultrasound, Magnetic Resonance Imaging (MRI) and Tomography are the other methods to diagnose breast cancer using Ionized radiation, which harms young women patients below 40 years. Microwave imaging can be used to distinguish between healthy and malignant tissues because it is a non-ionizing and potentially low-cost imaging method. When the dielectric properties of normal breast tissue and malignant breast tissue differ, a scattering or reflected wave can be generated by microwave imaging. An antenna is used to inject microwave signals into the breast. An antenna receiving a backscattered signal from cancerous cells receives a different signal than an antenna receiving a backscattered signal from normal breast tissue [22]. Therefore, antennas can detect breast cancer early with low-cost, no-pain, no-harmful radiation and locate malignant cells in any breast area more accurately than the above technique. Several simple and compact antennas were designed and developed for breast cancer detection. Patch antennas are particularly useful since they are compact and relatively light when mounted over the breast. Several antennas were designed in past research work for breast cancer detection; for example, a conventional patch antenna is designed, which operates at 2.4 GHz with different modified ground structures and measures only the electrical distribution of the antenna to detect cancerous tissue. In contrast, SAR, the most important parameter, is not measured, which helps in human safety [15]. In this paper [23], a compact slotted patch antenna for breast cancer detection is designed to operate at 8.45 GHz, where only the antenna's electrical distribution, gain and directivity are concentrated. In contrast, SAR for human safety is not measured. In [24], the circular patch antenna for breast cancer detection with two phantoms is compared. An elliptical planar ultra-wideband antenna is designed for breast cancer detection [25]; even though the wide band of frequency 1.5 GHz to 7 GHz is achieved in this antenna, SAR value measurement is missing, which makes it not suitable for the detection of cancer in human being as a safety measure is considered. Also, the shape of the phantom is cubic, which may result in appropriate results. In [26], the author designed a planar ultra wideband patch antenna array for breast tumor detection. It achieves a wide frequency range of 2.3 GHz - 11 GHz with a bandwidth of 8.4 GHz with 16 antennas in an array fashion. These arrays of antennas will occupy more space, and also, the SAR value is not identified in this paper, which makes to think whether this is suitable for detecting breast cancer in human beings. Due to security concerns since the antenna will operate over the torso, this paper utilizes a 20×15 mm^2 compact patch antenna to locate cancerous tumors inside the breast. The breast is designed to mimic a real human breast to ensure error-free results. Additionally, tissue properties are considered since microwave imaging relies on tissue electrical properties. Microwave imaging, especially with the proposed rectangular antenna embedded with a complementary split-ring resonator, stands out for its wide bandwidth, compact size, stable radiation pattern, and accurate tumor localization capabilities, offering a non-invasive, low-cost, and safe approach for early breast cancer detection. The paper is divided and discussed in 6 main sections. Section II discusses how to design the antenna & the breast phantom and how to simulate the antenna. Section III presents the antenna parameters for breasts with and without tumors. Section IV compares the proposed antenna results with other reported results. In section V, the fabrication of an antenna is discussed and measured and simulated results are compared. Finally, section VI concludes the paper with a brief overview of research.

2 RESEARCH METHOD

2.1 Design of Multiband Textile Antenna

The proposed textile based multiband rectangular patch antenna, embedded with a complementary split ring resonator, is designed using CST EM software. The structure was designed and fabricated on a Jean substrate with a loss tangent of 0.025, a dielectric constant of 1.7, and a thickness (h) of 2 mm. Fig. 1 depicts the proposed structure in five different configurations. 1. A simple rectangular textile antenna is designed to operate at 7 GHz at level 1. At level 2, the ground is reduced to match resonance with impedance matching. In level 3, an additional capacitance is introduced to achieve perfect impedance matching where the antenna resonates at 6 GHz. Then in configuration 4, a truncation has been carried out in patch to achieve wider bandwidth up to 10 GHz. Then in level 5, a CSRR is introduced to achieve multiband frequencies at 2.4 GHz, 5.8 GHz and 6.4 GHz, respectively. Parameter values are listed in Tab. 1. The proposed antenna operates at multiband frequencies at 1.75 GHz to 2.87 GHz with 2.45 GHz as resonant frequency, 4.79 GHz to 5.89 GHz, which resonates at 5.45 GHz and 6.37 GHz to 6.58 GHz, which resonates at 6.4 GHz.

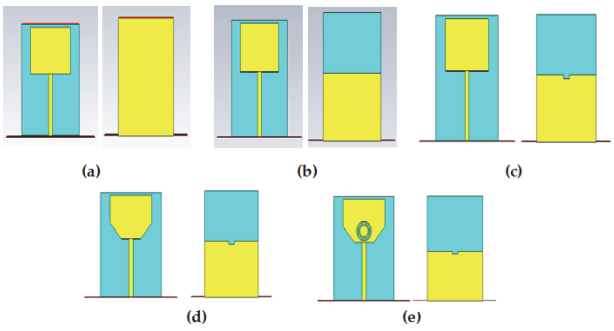

Figure 1 Evolution of Multiband Textile Antenna: (a) Level-1 Rectangular Seed antenna, (b) Level-2, Reduced ground structure, (c) Level-3 Reduced ground with slot, (d) Level-4 Truncated patch and (e) Level-5 Truncated patch with CSRR Embedded.

In Level 2, impedance matching is achieved with the reduction in the ground, and there is a frequency level shift because of the ground inductance reduction. A slot is introduced in level 3 to indicate the addition of capacitance in the ground, which allows the antenna to match its impedance perfectly. In level 4, a truncation in the patch creates wider bandwidth by combining two higher nodes obtained in level 3. Further, to achieve multiband frequency, a complementary split ring resonator is introduced in level 5. These two rings will change the current path based on their dimensions. In this way, the antenna resonates at 5.8 GHz and 6.3 GHz, respectively.

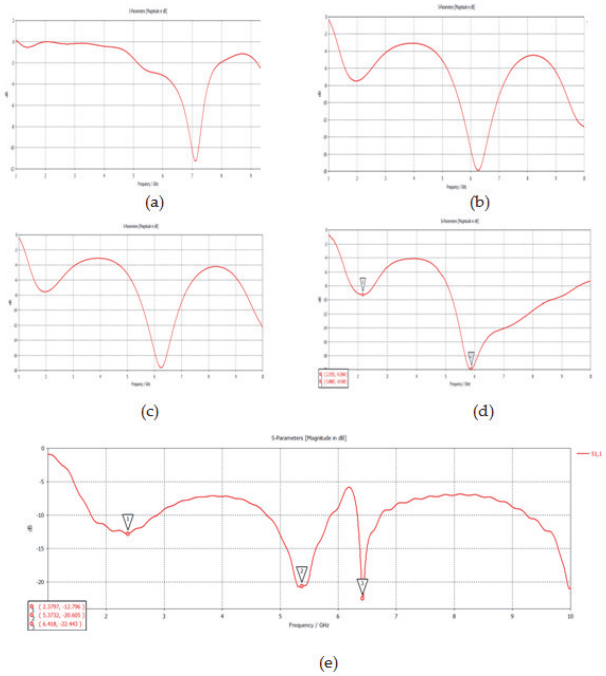

Figure 2 S11 - Measurements at various levels of configuration: (a) Level - 1, (b) Level - 2, (c) Level - 3, (d) Level - 4 and (e) Level - 5.

In the proposed antenna, the level 1, a rectangular radiating element, has a size of $wp \times lp$ and is mounted on a jean substrate. Conversely, it has a ground plane that measures $ws \times ls$. To design the antenna, we use the patch antenna equation, as shown below.

$$W = \frac{c}{2f_r}\sqrt{\frac{2}{\varepsilon_r + 1}} \tag{1}$$

$$L = \frac{c}{2f_r\sqrt{\varepsilon_{eff}}} - 2\Delta L \tag{2}$$

$$\varepsilon_{eff} = \frac{\varepsilon_r + 1}{2} + \frac{\varepsilon_r - 1}{2}\left[1 + \frac{12h}{W}\right]^{\frac{-1}{2}} \tag{3}$$

$$\Delta L = 0.41h\frac{\left(\varepsilon_{eff} + 0.3\right)}{\left(\varepsilon_{eff} - 0.258\right)}\frac{\left(\frac{W}{h} + 0.264\right)}{\left(\frac{W}{h} + 0.8\right)} \tag{4}$$

where: W - Width of the patch, L - Length of the patch, ΔL - Actual increase in length due to fringing, ε_{eff} - Effective dielectric constant, ε_r - dielectric constant of the substrate, c - Speed of the light, h - substrate height.

Table 1. Textile Antenna Parameter details (in mm)

Layers	Material	Parameters / mm
Patch	Copper	$W_p = 20$, $l_p = 15$, $l_{p1} = 9.40$, $l_{p2} = 7.78$ mm
Substrate	Jean	$W_s = 29$, $l_s = 36$, $h = 2$
Ground	Copper	$W_g = 29$, $l_g = 17$
Feed	Copper	$W_f = 2$, $l_f = 20$

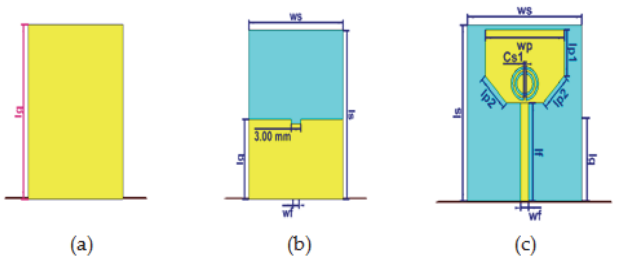

Figure 3 Geometry of Multiband Textile Antenna with CSRR engraving: (a) Level - 1 lg - Ground level, (b) Level - 3 - Reduced ground level with a slot, and (c) Geometrical dimensions of the antenna.

In level - 2, to match the impedance, the ground length of 36 mm in level - 1, as shown in Fig. 3a, is reduced to 17 mm, as shown in Fig. 3b. Hence, it has a wide bandwidth from 1.56 GHz to 2.54 GHz with a bandwidth of 1.02 GHz and 4.76 GHz to 8 GHz with a bandwidth of 3.76 GHz and also resonates at 1.96 GHz and 6.28 GHz respectively, as shown in Fig. 2b. The ground is then slotted; this changes the current path, reduces induction and adds capacitance, resulting in a smaller impedance bandwidth. Level 3 has multiband operations from 1.2 GHz to 3 GHz, from 5.76 GHz to 7.49 GHz and 9 GHz to 11 GHz, as depicted in Fig. 2c. In level - 4, the radiating elements are truncated, which allows the two high-frequency nodes in level 3 to combine and make a wider range of frequencies from 5.08 GHz to 10 GHz, as shown in Fig. 2d. Finally, at level - 5, the CSRR is embedded in the rectangular radiating element at the maximum surface current. With the CSRR, a new resonance is created at 2.4 GHz and multiple bands between 4.08 GHz and 10 GHz, from 4.80 GHz to 6 GHz, which resonates at 5.8 GHz, respectively 6.20 GHz to 6.81 GHz, which resonates at 6.42 GHz, and 9.66 GHz to 10.8 GHz that resonate at 10 GHz. Hence, the proposed antenna operates at multiband with center frequencies 2.4 GHz, 5.8 GHz and 66.42 GHz. ISM band frequency range is 2.4 to 2.5 GHz, 5.725 to 5.825 GHz, 5.925 GHz to 6.425 GHz, and 6.175 GHz to 7.125 GHz. This range is achieved after CSRR is engraved in the radiating patch. Reducing the ground length achieves a reasonable impedance bandwidth and ISM band frequency. An analysis of its corresponding data provided in Fig. 5 shows that lg = 17 mm is the ideal dimension for achieving maximum impedance bandwidth and reaching the ISM band. Hence, the ground value lg = 17 mm is chosen for the final fabrication.The chosen dimensions and configurations for the antenna slots were based on optimizing impedance matching, bandwidth, and resonance frequencies across multiple frequency bands, ensuring efficient electromagnetic wave propagation and reception for effective breast cancer detection.

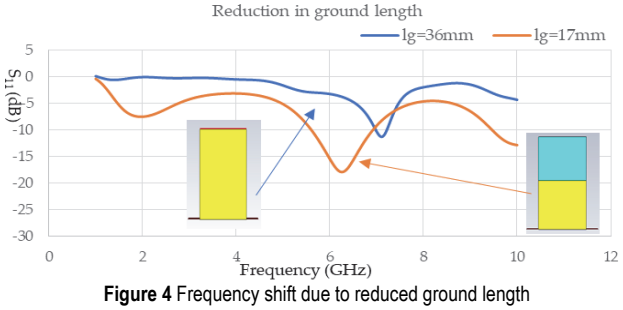

Figure 4 Frequency shift due to reduced ground length

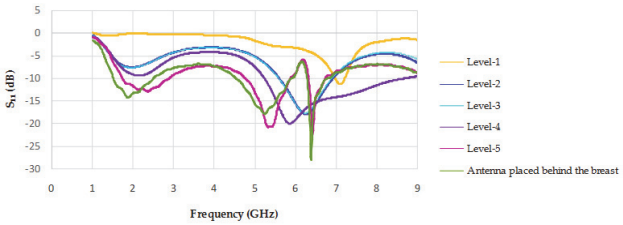

Figure 5 Return loss (S11) - at various levels

2.2 Designing of Breast Phantom

Breasts should be designed so they are as close to human breasts as possible to get reliable results and closer to practical value. Thus, an actual breast with a tissue composition is designed in this paper. During creation of the breast, it is important to maintain its tissue properties. A breast consists of two biological tissue layers, namely skin & fat, as shown in Fig. 6a. The total circumference and height of the breast are 56 mm and 60 mm, respectively.

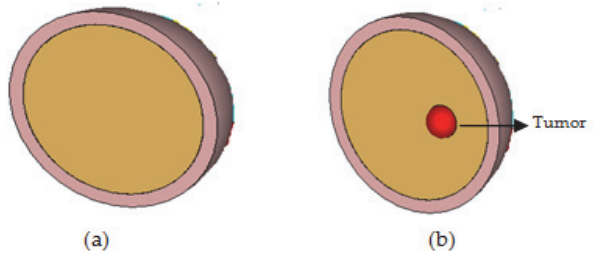

Figure 6 Breast Phantom Design: (a) Healthy breast, and (b) Affected breast

Table 2 Properties of the Breast Phantom

Layer	Diameter / mm	Property
Skin	60 mm	Epsilon = 3, Mu = 1, Electrical Conductivity = 0.856 s/m, Rho = 1100 kg/m^2, Thermal Conductivity = 0.29 W/K/m, Specific Heat = 3500 J/K/kg, Diffusivity = 7.61039e-08 m^2/S, Bloodflow = 9100 W/K/m^3, Metabolic Rate = 1620 W/m^3
Fat	56 mm	Epsilon = 3, Mu =1 , Electrical Conductivity = 0.4 s/m, Rho = 910 kg/m^3, Thermal Conductivity = 0.201 W/K/m, Specific Heat = 2.5 kJ/K/kg, Diffusivity = 8.83516e-08 m^2 /S, Bloodflow = 1700 W/K/m^3 , Metabolic Rate = 300 W/m^3

2.2 Simulation Set-up

Initially, the textile antenna was designed and evaluated in an open environment, and resonance frequencies were found at 2.452 GHz, 5.8 GHz, and 6.42 GHz.

Figure 7 Textile Antenna placed behind the affected breast (a) Perspective View, and (b) Side view of antenna placed at 10 mm behind the breast

As the antenna is about to be used to detect breast cancer, the antenna will be placed behind the affected breast at a distance of 10 mm since the effect of the human body should not affect the antenna's performance, as shown in Fig. 7. For affected breast designing, a tumor (dielectric conductivity = 4), with a 10 mm radius is fitted inside the breast's glandular tissue.

3 RESULT ANALYSIS

At first, the antenna is evaluated in an open environment. CST software simulates its S11 measurement, e-plane, h-plane, and surface current distribution. Then the antenna is placed over the affected breast tissue and healthy breast tissue, and the results are compared.

3.1 *S* - Parameter Measurement

The above result shows that antenna gain is not affected even when placed behind the human body, and it indicates that the antenna resonates at ISM band frequency range 2.4 GHz, 5.87 GHz, and 6.42 GHz, whereas there is a shift in frequency of 2.4 GHz to 2.01 GHz.

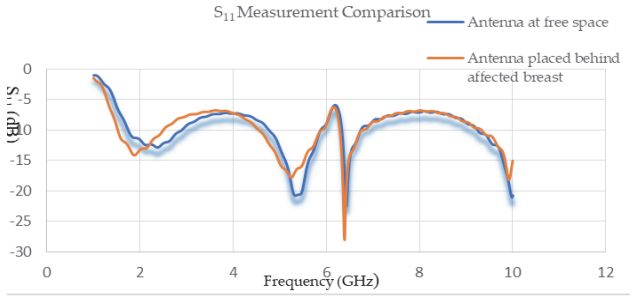

Figure 8 S - Parameter measurement analysis

3.2 Far Field Analysis for Tumor Detection

The antenna's electrical field intensity shown in Fig. 9, current density shown in Fig. 10 and magnetic field intensity, as shown in Fig.11, are scrutinized for 2.01 GHz and 5.8 GHz in search of the location of the defective cells.

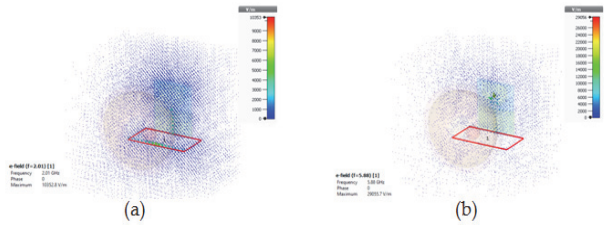

Figure 9 Electric Field Intensity: (a) e-plane at 2.01 GHz, (b) e-plane at 5.88 GHz

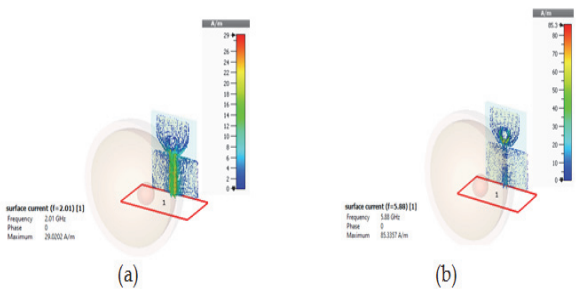

Figure 10 Surface Current Density at various frequencies: (a) 2.01 GHz, (b) 5.88 GHz

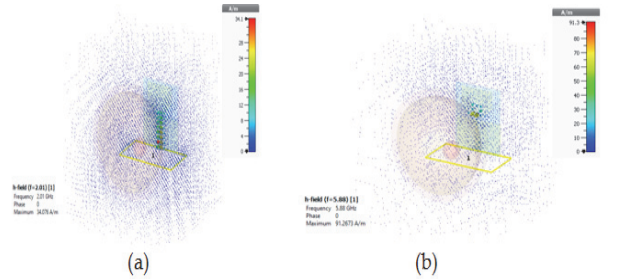

Figure 11 Magnetic Field Intensity: (a) h-plane at 2.01 GHz, (b) h-plane at 5.88 GHz

Table 3 Summary of Electric Field Intensity, Magnetic Field Intensity and Surface Current Density at two different frequencies

Description	Electric Field Intensity / V/m	Magnetic Field Intensity / A/m	Surface Current Density / A/m	Frequency / GHz
Without tumor	8682.52	47.354	39.48	2.01
With tumor	10352.8	34.076	29.02	2.01
Without tumor	38694	157.629	133.77	5.88
With tumor	29055.7	91.2673	85.33	5.88

From the above table, the breast is cancer-free if the achieved electrical properties match those of a normal breast, but if the obtained value does not match, there are cancerous cells in the breast.

3.3 Radiation Pattern Analysis

The radiation patterns of antennas are shown in 1-D polar views and 3-D views, respectively.

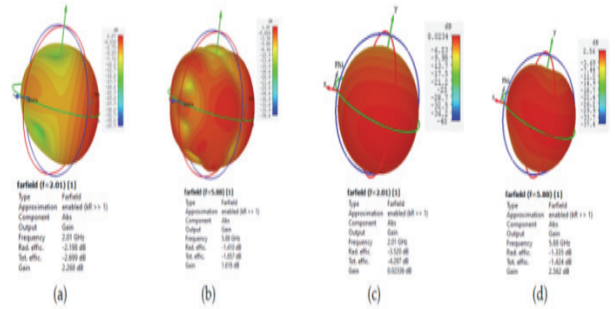

Figure 12 3-D radiation patterns of an antenna: (a) at 2.01 GHz without tumor, (b) at 5.88 GHz without tumor, (c) at 2.01 GHz with tumor, and (d) at 5.88 GHz with tumor

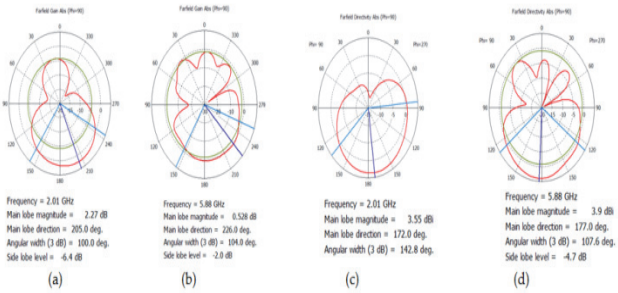

Figure 13 1-D radiation patterns of an antenna: (a) at 2.01 GHz without tumor, (b) at 5.88 GHz without tumor, (c) at 2.01 GHz with tumor, and (d) at 5.88 GHz with tumor

From the above Fig. 13, it is indicated there is a maximal magnitude, corresponding to 3.55 dBi at 2.01 GHz and 3.9 dBi at 5.88 GHz, when it operates over the breast with a tumor and a minimum magnitude, corresponding to 2.27 dBi and 0.528 dBi at 2.01 GHz and 5.88 GHz, respectively, when it operates over a breast without a tumor.

3.4 Specific Absorption Rate Analysis

An essential parameter to consider is the Specific Absorption Rate (SAR), an indicator of patient safety. It refers to how much electromagnetic energy from near-side sources is absorbed by nearby body tissues [27]. Patient safety dictates that the antenna's SAR values are calculated at the center frequency of the breasts. An antenna with an input power of one milliwatt is used to measure the SAR for one gram of body tissue. The obtained values of SAR fall within the maximum tolerable range (1.6 W/kg) as per government and industry standards without a tumor.

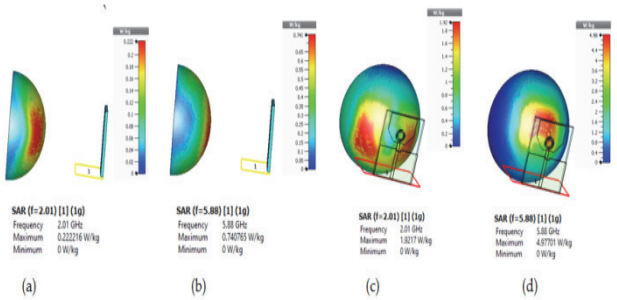

Figure 14 SAR analysis at different frequency: (a) at 2.01 GHz without tumor, (b) at 5.88 GHz without tumor, (c) at 2.01 GHz with tumor, and (d) at 5.88 GHz with tumor

Without the tumor, the SAR value is 0.222 W/Kg and 0.741, which is below the IEEE standards, but due to the tumor in the breast, the antenna at 2.01 GHz and 5.88 GHz indicates the SAR value is high, 1.9217 W/kg and 4.97 W/kg respectively. The high value of SAR indicates the presence of tumor in both frequencies.

Table 4 Averaged SAR values for 1g and coordinates in the heterogeneous breast without tumor

Frequency / GHz	1 gm Analysis	
	Maximum SAR / W/Kg	Maximum at (*X*, *Y*, *Z*) mm
2.01	0.222	(–15.990, –1.500, 58.974)
5.88	0.741	(–1.000, –8.250, 55.105)

Table 5 Averaged SAR values for 1g and coordinates in heterogeneous breast with tumour

Frequency / GHz	1gm Analysis	
	Maximum SAR / W/Kg	Maximum at (*X*, *Y*, *Z*) mm
2.01	1.922	(14.75, 5.542, 28.964)
5.88	4.97	(0.000, 7.600, 25.093)

A UWB signal is used to radiate the heterogeneous breast phantom. Maximum SAR and coordinates of Maximum SAR are obtained for 2.01 and 5.88 GHz resonant frequencies, respectively. Tab. 4 shows the Maximum SAR and coordinate values for a breast phantom without a tumor in 1g analysis. Similarly, Tab. 5 shows the total Maximum SAR and the coordinates of Maximum SAR of a breast phantom with a tumor of a radius of 10 mm. In all frequency ranges, the maximum SAR is always higher in breast phantoms with tumor than those without tumor. The research extensively explores the concept of Specific Absorption Ratio (SAR) by analyzing its values at different frequencies and correlating them with

tumor presence. It effectively demonstrates the potential of the proposed antenna for accurate tumor localization through maximum SAR values, showcasing higher SAR values in breast phantoms with tumors compared to those without, indicating the antenna's capability for precise tumor detection and localization.

4 FABRICATION OF ANTENNA

Initial fabrication begins with a mask containing the design's negative. The structure with copper-clad jeans is laminated with an inverted negative photoresist film after it has been cleaned with acetone and dried. UV light is used to expose the mask to the laminated structure. It is then dissolved in a sodium carbonate developer solution and etched with a ferric chloride solution. As the photoresist hardens, sodium hydroxide is applied to remove it. Photolithography and chemical etching are used to manufacture the antenna. The study presents a comprehensive overview of the design and fabrication details of the proposed antenna, including the utilization of a jean substrate with dimensions of $20 \times 15 \times 2$ mm^3, and highlights its multiband operation, compact size, and stable radiation pattern, demonstrating meticulous attention to both material selection and dimensional specifications. Fig. 15 shows simulated and measured radiation patterns in the E-plane and H-plane. The proposed structure exhibits stable radiation patterns across all resonating bands. It is evident from the figure that the textile-based rectangular multiband antenna has an omnidirectional H-plane pattern and an eight-shaped dipole E-plane pattern.

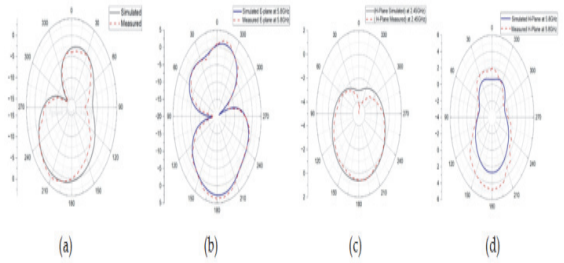

Figure 15 E-Plane and H-Plane (Simulated vs. Measured) at various resonant frequencies: (a) E-plane at 2.01 GHz (b) E-Plane at 5.8 GHz (c) H-Plane at 2.01 GHz (d) H-Plane at 5.8 GHz

Figure 16 (a) The Anechoic chamber set-up, (b) Measurements are carried out using a VNA Agilent N5247A (Microwave network analyzer) on the prototype that has been fabricated

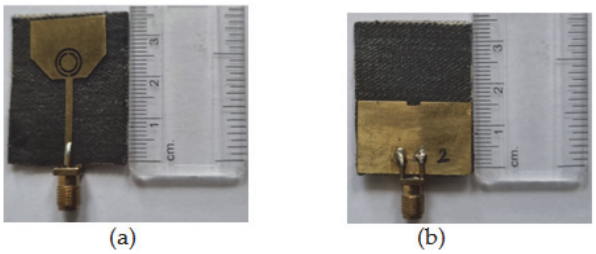

Figure 17 Fabricated Prototype of Antenna (a) Front view, and (b) Back view

The measured result is compared with the simulated ones and presented in Fig. 18. The deviation between the results is due to the connector error at high frequency and fabrication inadequacy. The antenna's efficiency and bandwidth were evaluated using electromagnetic simulation software for initial design and experimental setups with vector network analyzers in an anechoic chamber for validation, ensuring comprehensive assessment for practical application suitability.

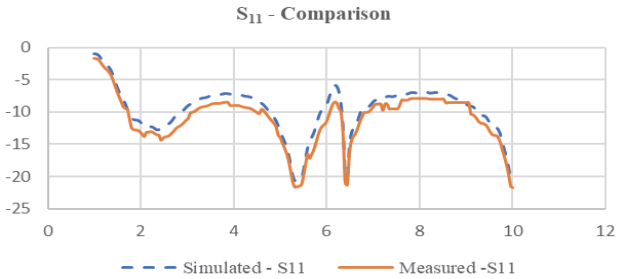

Figure 18 Simulated S11 Vs Measured S11

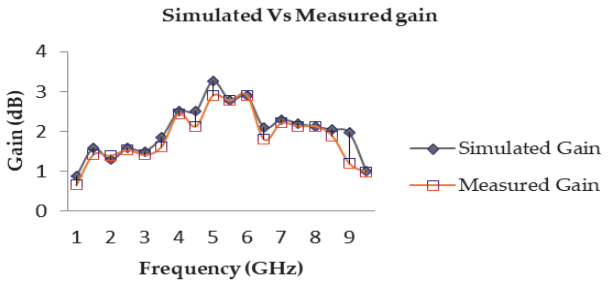

Figure 19 Simulated gain Vs Measured gain

All resonating bands maintain gains above 1.7 dBi, with the proposed and simulated gains on par. The above figure shows a maximum gain of 3.25 dBi. The measured results of the designed antenna exhibit robustness, aligning well with the simulated data. Its notable features, including multiband operation, compact size, stable radiation pattern, and gain exceeding 3.25 dBi, collectively contribute to its suitability for breast cancer imaging and wireless body area networks (WBAN) within the ISM band by ensuring reliable and accurate signal transmission and reception, essential for effective diagnosis and monitoring without compromising patient safety or comfort.

5 CONCLUSION AND FUTURE SCOPE

In this article, a tiny rectangular monopole microstrip patch antenna embedded with CSRR operating at a multiband frequency range for breast cancer detection is designed and fabricated. An antenna was placed over a healthy and a cancer-affected breast to test its efficiency

and parameters. Despite its compact size, the proposed antenna delivers a bandwidth of 2 GHz to 10 GHz. According to the simulated data above, the maximum SAR values (1.922 and 4.97) in the breast phantom with tumors were higher than those in the breast without tumors (0.222 and 0.741). At the tumor location of (–0.75, –2,0), the tumor radius of 10mm was analyzed with different resonance frequencies, including 2.01 and 5.88 GHz. The maximum SAR coordinates are very close to the actual tumor location. Therefore, the maximum SAR value indicates the presence of tumor in the breast phantom which is higher than the breast without tumour. For both states of the breast (affected and healthy), simulation results are satisfactory for return loss, radiation pattern, surface current density, e-plane and h-plane calculations. Finally, SAR reveals patient safety in proximity to the antenna. So, considering antenna performance, it would be fruitful to use this antenna to detect breast cancer in real life. The proposed antenna has also been fabricated, and S11 measurement, gain, E-plane, and H-plane measured results were compared with simulated results, indicating that their values are the same with a slight shift in S11. Here are a few significant features of the proposed antenna, including its simple design, compact size, reasonable gain, impedance matching, and stable radiation pattern. Planned improvements include cost optimization, enhanced detection accuracy via signal processing, and miniaturization for wearability. Extensive clinical trials will validate real-world efficacy, refining the design based on user feedback.

6 REFERENCES

[1] Ganesan, R., Panchavarnam, M.V., & Thangaiyan, J. (2023). Split Ring Resonator Inspired Dual-Band Monopole Antenna for ISM, WLAN, WIFI, and WiMAX Application. *Tehnički vjesnik, 30*(5), 1533-1538. https://doi.org/10.17559/TV-20230210000344

[2] Orhan, A. & Mesud, K., (2022).The Effect of the Co-Planar Structure on HPBW and the Directional Gain at the Square Patch Antenna around ISM 2450 MHz. *Technical Gazette, 29*(4), 1120-1125. https://doi.org/10.17559/TV-20190423010908

[3] Kaur, G., Kaur, A., Toor, G., Dhaliwal, B., & Pattnaik, S. (2015). Antennas for biomedical applications. *Biomedical Engineering Letters, 5*(3), 203-212. https://doi.org/10.1007/s13534-015-0193-z

[4] Vidya, V. D. & Suvarna, S. C. (2020). Microstrip Antennas used for Non invasive Determination of Blood Glucose Level. *2020 4th International Conference on Intelligent Computing and Control Systems (ICICCS), Madurai, India*, 720-725. https://doi.org/10.1109/ICICCS48265.2020.9120873

[5] Ahmed, A., Ur-Rehman, M., & Abbasi, Q. H. (2018). Miniature implantable antenna design for blood glucose monitoring. *International Applied Computational Electromagnetics Society Symposium*, *IEEE*, 1-2. https://doi.org/10.23919/ROPACES.2018.8364219

[6] El Abbasi, M., Madi, M., Jelinek, H., & Kabalan, K. (2022). Wearable Blood Pressure Sensing Based on Transmission Coefficient Scattering for Microstrip Patch Antennas. *Sensors, 22*(11), 3996. https://doi.org/10.3390/s22113996

[7] Lin, H. D., Lee, Y. S., & Chuang, B. N. (2012). Using dual-antenna nanosecond pulse near-field sensing technology for non-contact and continuous blood pressure measurement. *Proc. Ann. Int. Conf., San Diego*, 219-222, https://doi.org/10.1109/embc.2012.6345909

[8] Angelin, H. & Kumar, K. M. (2017). Brain tumor detection using metamaterial based microstrip patch antenna. *Int. Res. J. Eng. Technol*., 3340-3344.

[9] Singh, T., Singh, S., Singh, M., & Kaur, R. (2019). Design of patch antenna to detect brain tumor. *Proc. Int. Conf. Issues Challenges Intell. Comput. Techn. (ICICT)*, 1-6. https://doi.org/10.1109/ICICT46931.2019.8977631

[10] Raihan, R., Bhuiyan, M. S. A., Hasan, R. R., Chowdhury, T., & Farhin, R. (2017). A wearable microstrip patch antenna for detecting brain cancer. *Proc. IEEE 2nd Int. Conf. Signal Image Process. (ICSIP)*, 432-436. https://doi.org/10.1109/SIPROCESS.2017.8124578

[11] Al-Nahiun, S. A. K., Mahbub, F., Islam, R., Akash, S. B. R., Hasan, R., & Rahman, M. A. (2021). Performance analysis of microstrip patch antenna for the diagnosis of brain cancer & tumor using the fifth-generation frequency band. *Proc. IEEE Int. IoT, Electron. Mechatronics Conf. (IEMTRONICS)*, 1-6. https://doi.org/10.1109/IEMTRONICS52119.2021.9422503

[12] Çalışkan, R., Gültekin, S. S., Uzer, D., & Dündar, Ö. (2015). A Microstrip Patch Antenna Design for Breast Cancer Detection. *Procedia - Social and Behavioral Sciences, 195*, 2905-2911. https://doi.org/10.1016/j.sbspro.2015.06.418

[13] Rao, P. K. & Mishra, R. (2019). Ultra-wide-band Flexible Antenna for Breast Cancer Detection. *IEEE 5th International Conference for Convergence in Technology*, 1-4. https://doi.org/10.1109/I2CT45611.2019.9033875

[14] Aziz, A., Ahmad, D., Shila, T. A., Rana, S., Hasan, R. R., & Rahman, M. A. (2019). On-Body Circular Patch Antenna for Breast Cancer Detection. *2019 IEEE International Electromagnetics and Antenna Conference (IEMANTENNA)*, *Vancouver*, 29-34. https://doi.org/10.1109/IEMANTENNA.2019.8928707

[15] Hammouch, N. & Ammor, H. (2018). Smart UWB antenna for early breast cancer detection. *ARPN Journal of Engineering and Applied Sciences, 13*, 3803-3808.

[16] Miller, K. D., Nogueira, L., Mariotto, A. B. , Rowland, J. H., Yabroff, K. R., Alfano, C. M., Jemal, A., Kramer, J. L., & Siegel, R. L. Cancer treatment and survivorship statistics. CA, *Cancer J. Clinicians, 69*, 363-385. https://doi.org/10.3322/caac.21565

[17] Capuano, R., Catini, A., Paolesse, R., & Di Natale, C. (2019). Sensors for lung cancer diagnosis. *J. Clin. Med., 8*(2), 235. https://doi.org/10.3390/jcm8020235

[18] Sung, H., Ferlay, J., Siegel, R. L., Laversanne, M., Soerjomataram, I., Jemal, A., & Bray, F. (2021). Global Cancer Statistics 2020, GLOBOCAN Estimates of Incidence and Mortality Worldwide for 36 Cancers in 185 Countries. *CA Cancer J Clin, 71*(3), 209-249. https://doi.org/10.3322/caac.21660

[19] DeSantis, C., Siegel, R., Bandi, P., & Jemal, A. (2011). Breast cancer statistics. *CA Cancer J Clin., 61*(6), 409-418. https://doi.org/10.3322/caac.20134

[20] *International Agency for Research on Cancer*. India Source: Globocan 2020.2021, 11.

[21] Løberg, M., Lousdal, M. L., Bretthauer, M., & Kalager, M. (2015). Benefits and harms of mammography screening. *Breast Cancer Res., 17*(1), 63. https://doi.org/10.1186/s13058-015-0525-z

[22] Zhang, H., Arslan, T., & Flynn, B. (2013). A single antenna-based microwave system for breast cancer detection: Experimental results. *Loughborough Antennas & Propagation Conference (LAPC)*, 477-481. https://doi.org/10.1109/LAPC.2013.6711945

[23] Islam, M. T., Samsuzzaman, M., Rahman, M. N., & Islam, M. T. (2018). A compact slotted patch antenna for breast tumor detection .*Microw. Opt. Technol. Lett., 60(7)*, 1600-1608. https://doi.org/10.1002/mop.31215

[24] Gong, F., Wei, Z., Cong, Y., Chi, H., Yin, B., & Sun, M. (2017). Analysis of SAR distribution in human head of

antenna used in wireless power transform based on magnetic resonance. *Technol Health Care, 25*(S1), 387-397. https://doi.org/10.3233/thc-171342

[25] Mansoor, F., Tan, T., & Latif. S. I. (2017). The performance of an Ultra-wideband elliptical ring monopole antenna with a humanoid breast phantom.. *IEEE International Symposium on Antennas and Propagation & USNC/URSI National Radio Science Meeting*, 105-106. https://doi.org/10.1109/APUSNCURSINRSM.2017.8072095

[26] Hossain, A., Islam, M. T., Islam, M. T., Chowdhury, M. E. H., Rmili, H., & Samsuzzaman, M. (2020). A Planar Ultrawideband Patch Antenna Array for Microwave Breast Tumor *Detection. Materials, 13*(21), 4918. https://doi.org/10.3390/ma13214918

[27] Roja, G., Maheswara Venkatesh, P., & Jayasankar, T., (2023). Split Ring Resonator Inspired Dual-Band Monopole Antenna for ISM, WLAN, WIFI, and WiMAX Application. *Technical Gazette, 30*(5), 1533-1538. https://doi.org/10.17559/TV-20230210000344

[28] Alsharif, F. & Kurnaz, C. (2018). Wearable microstrip patch ultra wide band antenna for breast cancer detection. *Proceedings of the 2018 41st International Conference on Telecommunications and Signal Processing (TSP)*, 4-6. https://doi.org/10.1109/TSP.2018.8441335

[29] Srikanth, B. S., Gurung, S. B., Manu, S., Gowthami, G. N., Ali, T., & Pathan, S. (2020). A slotted UWB monopole antenna with truncated ground plane for breast cancer detection. *Alex. Eng. J., 59*(5), 3767-3780. https://doi.org/10.1016/j.aej.2020.06.034

[30] Marwa, S., Bassem, J., Hugo, D., Ali, G., & Paulo, M. M. (2022). Metamaterial Vivaldi Antenna Array for Breast Cancer Detection. *Sensors***,** *22*(10), 3945. https://doi.org/10.3390/s22103945

[31] Çalışır, B. & Akbal, A. (2022). A New RF Satellite Link Analyzing and Antenna Effect on Satellite Communication. *Tehnički glasnik, 16*(4), 550-556. https://doi.org/10.31803/tg-20220405153200

[32] Ermiş, S. & Demirci, M. (2023). Improving the Performance of Patch Antenna by Applying Bandwidth Enhancement Techniques for 5G Applications. *Tehnički glasnik, 17*(3), 305-312. https://doi.org/10.31803/tg-20220819001236

Contact information:

M. FAHMITHA BANU, Assistant Professor
(Correspondig author)
Dept. of ECE,Dr.NGP Institute of Technology,
Coimbatore, Tamilnadu, India
E-mail: fahmithaashok@yahoo.com

B. ARUNA DEVI
Dept. of ECE, Dr.NGP Institute of Technology,
Coimbatore, Tamilnadu, India
E-mail: arunadevidrngpit@rediffmail.com